BNL-112549-2016-JA

An exact variational method to calculate rovibrational spectra of polyatomic molecules with large amplitude motion

Hua-Gen Yu

Submitted to Journal of Chemical Physics

August 2016

Chemistry Department

Brookhaven National Laboratory

U.S. Department of Energy
USDOE Office of Science (SC),
Basic Energy Sciences (BES) (SC-22)

Notice: This manuscript has been authored by employees of Brookhaven Science Associates, LLC under Contract No. DE- SC0012704 with the U.S. Department of Energy. The publisher by accepting the manuscript for publication acknowledges that the United States Government retains a non-exclusive, paid-up, irrevocable, world-wide license to publish or reproduce the published form of this manuscript, or allow others to do so, for United States Government purposes.

DISCLAIMER

This report was prepared as an account of work sponsored by an agency of the United States Government. Neither the United States Government nor any agency thereof, nor any of their employees, nor any of their contractors, subcontractors, or their employees, makes any warranty, express or implied, or assumes any legal liability or responsibility for the accuracy, completeness, or any third party's use or the results of such use of any information, apparatus, product, or process disclosed, or represents that its use would not infringe privately owned rights. Reference herein to any specific commercial product, process, or service by trade name, trademark, manufacturer, or otherwise, does not necessarily constitute or imply its endorsement, recommendation, or favoring by the United States Government or any agency thereof or its contractors or subcontractors. The views and opinions of authors expressed herein do not necessarily state or reflect those of the United States Government or any agency thereof.

(Submitted to *J. Chem. Phys.*, 2016)

An exact variational method to calculate rovibrational spectra of polyatomic molecules with large amplitude motion

Hua-Gen Yu[1]

Division of Chemistry, Department of Energy and Photon Sciences,

Brookhaven National Laboratory, Upton, NY 11973-5000, USA

(August 3, 2016)

Abstract

We report a new full-dimensional variational algorithm to calculate rovibrational spectra of polyatomic molecules using an exact quantum mechanical Hamiltonian. The rovibrational Hamiltonian of system is derived in a set of orthogonal polyspherical coordinates in the body-fixed frame. It is expressed in an explicitly Hermitian form. The Hamiltonian has a universal formulation regardless of the choice of orthogonal polyspherical coordinates and the number of atoms in molecule, which is suitable for developing a general program to study the spectra of many polyatomic systems. An efficient coupled-state (CS) approach is also proposed to solve the eigenvalue problem of the Hamiltonian using a multi-layer Lanczos iterative diagonalization approach via a set of direct product basis set in three coordinate groups: radial coordinates, angular variables, and overall rotational angles. A simple set of symmetric top rotational functions is used for the overall rotation whereas a potential-optimized discrete variable representation (PO-DVR) method is employed in

[1]E-mail: hgy@bnl.gov

radial coordinates. A set of contracted vibrationally diabatic basis functions is adopted in internal angular variables. Those diabatic functions are first computed using a neural network iterative diagonalization method (NNiDM) based on a reduced-dimension Hamiltonian but only once. The final rovibrational energies are computed using a modified Lanczos method for a given total angular momentum J, which is usually fast. Two numerical applications to CH_4 and H_2CO are given, together with a comparison with previous results.

1 Introduction

Calculating rovibrational spectra of polyatomic molecules is one major goal in chemical physics. During the past decades, great progress has been made, e.g. see recent reviews.[1–5] Now full dimensional quantum dynamics calculations can be done for polyatomic molecules up to nine atoms using a nearly exact Hamiltonian.[6–12] It is not so difficult to compute vibrational spectra of polyatomic molecules up to six atoms[2,4,13–16] with the help of the parallel computing of supercomputers. If the molecule of interest is rigid, the Eckart-Watson Hamiltonian (usually based on normal coordinates) is often used. Its rovibrational spectrum can be efficiently studied by using a vibrational self-consistent filed (VSCF)[17,18] based approach, such as the vibrational configuration interaction (VCI)[13,19] and vibrational coupled cluster (VCC) methods,[20,21] or the perturbation approach.[12,22] However, it is still difficult to calculate highly vibrationally excited states and/or to study molecules with large amplitude motion using these methods. For those systems, curvilinear coordinates[3,23–29] are better to describe the system dynamics, and the large amplitude motion is naturally taken into account. Since the choice of curvilinear coordinates, which determines the molecular Hamiltonian,[30,31] is generally system-dependent, dynamics calculations require specific techniques in order to be done efficiently. In particular, for large polyatomic molecular systems, a sophisticated basis contraction[32–38] based on sequential diagonalization and truncation strategy has to be utilized to deal with the resulting huge basis size. By using curvilinear coordinates, some benchmark calculations such as those on CH_4, CH_5^+, $H_5O_2^+$ and malonaldehyde have been excellently accomplished.[4,6–12,14,39–41]

Orthogonal polyspherical coordinates[3,5,28,42,43] are particularly useful curvilinear coordinates. They are widely used in quantum scattering chemical dynamics.[44] A set of orthogonal coordinates can be formed by a combination of Jacobi,[3] Radau[45] and orthogonal satellite vectors.[15,46] They provide a more flexible description to a variety of chemical bond molecules. In orthogonal polyspherical coordinates, the determined Hamiltonian has

several important merits except that large amplitude motion of molecules is well represented. Firstly, the Hamiltonian is very compact as there are only a few terms in the kinetic energy operator. There is no mixed partial derivative term between the radial and angular variables. This provides a great advantage in numerical calculations. The second important feature is that the structure of the Hamiltonian is independent of the choice of vectors except for the pre-factors in the kinetic energy operator. The pre-factors depend only on the masses of atoms but are associated vectors.[15,42] This important feature allows us to develop a general program for polyatomic molecules with a chosen number of atoms by using a relationship between the orthogonal vectors and the atomic Cartesian coordinates. Bramley and Carrington[42] programmed a DVR-Lanczos routine to calculate vibrational energy levels of four-atom molecules, and applied it to H_2CO and HOOH. By using the same strategy, Yu and Muckerman[47] developed a general variational algorithm to calculate vibrational energy levels of tetra-atomic molecules for a given potential energy surface, where a mixed grid/basis set was used. The algorithm has been applied to several semi-rigid and floppy molecules such as H_2CO, NH_3, CH_3^+, HOOH and the van der Waals molecule He_2Cl_2. Recently, the author has written a general problem-independent program (PetroVib) for pentaatomic molecules,[15] in which 21 sets of orthogonal polyspherical coordinates are implemented. The infrared transition intensities can be also calculated.[16] The program has been applied for computing the vibrational spectra of several rigid or floppy molecules[15,48,49] including CH_4, NH_4^+, CH_2OO, He_3Cl_2, and $H_3O_2^-$. Furthermore, by exploiting the merits of both normal modes and orthogonal polyspherical coordinates, Leforestier *et al*[43] proposed a Jacobi-Wilson method for semi-rigid molecules.

The partitioned structure of the Hamiltonian in orthogonal polyspherical coordinates is another wonderful advantage.[5] By exploring the partitioned structure, the full dimensional eigen-problem can be solved efficiently in a reduced-dimensional manner by dividing the coordinates into two groups: angular and radial coordinates. Two efficient contraction

algorithms[35,50] have been developed for vibrational state calculations. These algorithms were extended to compute the rovibrational energies via $\Omega-$ or $K-$dependent vibrational diabatic functions[36,51] in angular variables. Although the $\Omega-$ or $K-$dependent approaches are very accurate, the algorithms are less efficient. This is because one has to carry out $(J+1)$ times iterative diagonalizations for constructing those $\Omega-$ or $K-$dependent diabats for a given total angular momentum J. In order to avoid this drawback, a simple $K-$independent scheme was proposed by Wang and Carrington.[36] Numerical results showed that it is a very good approximation for CH_4.

There are many methods to calculate rovibrational states of molecules.[1,4,13,52] One common approach starts with pure vibrational states, and treats rotational motions as a perturbation. For instance, Csaszar and his co-workers[41] have used a product basis set of pure vibrational eigenstates and rotational Wigner functions to efficiently compute large numbers of rovibrational states of ketene. If the Coriolis couplings are not strong, it is a very good approach. This strategy was adapted by Wodraszka and Manthe[53] to incorporate with the time-dependent multiconfigurational Hartree (MCTDH) method for calculating rovibrational eigenstates of CH_2D. Nevertheless, such calculations have high memory costs as vibrational states and some related matrices have to be stored. Recently, Wang and Carrington[40] proposed a Coriolis coupling-minimized method for computing rovibrational levels of methane by using curvilinear internal vibrational coordinates and an Eckart frame.

In this work, we will develop an exact variational method to calculate the rovibrational spectra of polyatomic molecules for a given potential energy surface. It is a general iterative diagonalization algorithm in terms of orthogonal polyspherical coordinates. Here, we will fully explore the salient merits of orthogonal polyspherical coordinates. The theory will be described in Sec. 2, where the rovibrational Hamiltonian of system and multi-layer Lanczos iterative diagonalization method are given. Two numerical applications are illustrated in Sec. 3. The conclusion is summarized in Sec. 4.

2 Theory

2.1 Hamiltonian in orthogonal polyspherical coordinates

Recently, the orthogonal polyspherical coordinate approach becomes popular in rovibrational spectrum calculations,[8,15,28,36,39,42,43,47,54,55] e.g. see a recent excellent review.[3] In this subsection we will describe a universal Hamiltonian for a general polyatomic system with N atoms in a set of orthogonal polyspherical coordinates. A novel partitioned formulation of rovibrational Hamiltionian will be derived. By using the Hamiltonian, an iterative diagonalization method is then developed for calculationg rovibrational states. Since the algorithm is developed from the two-layer Lanczos method,[35,73] some essential descriptions of vibrational state calculations will be included for better understanding. We will start with a concise representation of Hamiltonian in the space-fixed (SF) frame.

In the absence of an external field, only $(N-1)$ independent vectors are required to describe an $N-$body system by removing the motion of the center of mass of molecule. These orthogonal vectors are denoted as $(\mathbf{r}_i,\, i = 1, 2, \cdots, (N-1))$. In spherical coordinates (r, θ^{SF}, ϕ), the Hamiltonian of the system can be written as[3,5,28,43]

$$\hat{H} = \sum_{i=1}^{N-1} \left(-\frac{\hbar^2}{2\mu_i r_i^2} \frac{\partial}{\partial r_i} r_i^2 \frac{\partial}{\partial r_i} + \frac{\hat{j}_i^2}{2\mu_i r_i^2} \right) + V(\{\mathbf{r}_i\}; \{\mathbf{x}_\eta\}) \tag{1}$$

with the angular momentum operator

$$\hat{j}_i^2 = -\hbar^2 \left(\frac{1}{\sin\theta_i^{SF}} \frac{\partial}{\partial\theta_i^{SF}} \sin\theta_i^{SF} \frac{\partial}{\partial\theta_i^{SF}} + \frac{1}{\sin^2\theta_i^{SF}} \frac{\partial^2}{\partial\phi_i^2} \right) \tag{2}$$

and the volume element

$$d\tau = \prod_{i=1}^{N-1} r_i^2 \sin\theta_i^{SF} dr_i d\theta_i^{SF} d\phi_i. \tag{3}$$

In Eq. (1), μ_i is the reduced mass associated with a vector $\mathbf{r}_i$, which only depends on the atomic masses. $V(\{\mathbf{r}_i\}; \{\mathbf{x}_\eta\})$ is the potential energy surface of the system, where the vectors $\mathbf{x}_\eta$ give the Cartesian coordinates of atom η in the SF frame.

Calculations will be carried out in the body-fixed (BF) frame. As usual, we select the vector $\mathbf{r}_{N-1}$ to be coincident with the BF z-axis, and the vector $\mathbf{r}_{N-2}$ to be in the xz plane

with a positive x direction in the BF frame. That is, the spherical angles of $\mathbf{r}_{N-1}$ and the azimuthal angle of $\mathbf{r}_{N-2}$ are zero, which result in $(3N-6)$ internal variables. They are defined by $(N-1)$ radial coordinates ($\mathbf{R} = \{r_1, r_2, \cdots, r_{N-1}\}$) and $(2N-5)$ angular variables ($\mathbf{Q}$), including $(N-2)$ polar angles $\{\theta_i\}$ and $(N-3)$ azimuthal angles $\{\varphi_j\}$ of the radial vectors in the BF frame. However, beyond four-body systems, the angular variables are not uniquely defined by this BF definition.[7,15,36] One has to use additional conventions to determine them. In this work, we will use convention A from Ref. [7], which was also used by other groups.[28,55] In this convention the relative azimuthal angles are defined as

$$\varphi_k = \phi_k - \phi_{N-2},\ k = 1, \cdots, N-3, \tag{4}$$

with the range of $\varphi_k \in [0, 2\pi]$. Fig. 1 shows the orthogonal polyspherical coordinates in the BF frame that are used in this work.

By using the $z-$component ($\hat{j}_z$) and ladder operators $\hat{j}_\pm$ of angular momentum[56]

$$\hat{j}_z = -i\hbar\frac{\partial}{\partial\phi}, \tag{5}$$

$$\hat{j}_\pm = \pm\hbar e^{\pm i\phi}\left(\frac{\partial}{\partial\theta} \pm i\cot\theta\frac{\partial}{\partial\phi}\right), \tag{6}$$

and the chain rules

$$\begin{cases} \frac{\partial}{\partial\phi_k} = \frac{\partial}{\partial\varphi_k},\ k = 1, \cdots, N-3 \\ \frac{\partial}{\partial\phi_{N-2}} = -\sum_{j=1}^{N-3}\frac{\partial}{\partial\varphi_j}, \end{cases} \tag{7}$$

we have derived the following rovibrational Hamiltonian

$$\hat{H} = \hat{H}_v + \hat{T}_{vr} \tag{8}$$

with

$$\hat{H}_v = \hat{T}_R(\mathbf{R}) + \hat{H}_Q(\mathbf{Q};\mathbf{R}), \tag{9}$$

$$\hat{T}_{vr} = \hat{T}^D_{r,CS} + \hat{T}^C_{r,CS}, \tag{10}$$

for $N-$atomic systems in the BF frame. Here, $\hat{T}_{vr}$ is the rotational kinetic energy operator including the rotation-vibrational couplings. It will be described below. $\hat{H}_v$ is the pure

vibrational Hamiltonian that only depends on the $3N-6$ internal coordinates. It is partitioned into two terms. $\hat{T}_R(\mathbf{R})$ is the kinetic energy operator in the radial coordinates. It is obtained by a summation of one dimensional (1D) Hamiltonian $\hat{h}(r_i)$, i.e.,[16]

$$\hat{T}_R(\mathbf{R}) = \sum_{i=1}^{N-1} [\hat{h}(r_i) - V_0(r_i)], \tag{11}$$

$$\hat{h}(r_i) = -\frac{\hbar^2}{2\mu_i r_i^2}\frac{\partial}{\partial r_i} r_i^2 \frac{\partial}{\partial r_i} + V_0(r_i). \tag{12}$$

Here, $V_0(r_i)$ is a 1D reference potential in r_i with its associated reduced mass μ_i. The another term is given by

$$\hat{H}_Q(\mathbf{Q};\mathbf{R}) = \hat{T}_Q(\mathbf{Q};\mathbf{R}) + V(\mathbf{Q},\mathbf{R}), \tag{13}$$

where the potential energy surface $V(\mathbf{Q},\mathbf{R})$ is expressed in the internal coordinates. $\hat{T}_Q(\mathbf{Q};\mathbf{R})$ is the kinetic operator in the internal angular coordinates. It can be written as[7,35]

$$\hat{T}_Q(\mathbf{Q};\mathbf{R}) = \sum_{i=1}^{N-1} f_i(r_i)\hat{T}_Q^{(i)}(\mathbf{Q}),\ f_i = \frac{1}{2\mu_i r_i^2}, \tag{14}$$

with

$$\hat{T}_Q^{(i)}(\mathbf{Q}) = \hat{j}_i^2,\ i = 1,\cdots,N-2, \tag{15}$$

$$\hat{T}_Q^{(N-1)}(\mathbf{Q}) = \sum_{i=1}^{N-2} \hat{j}_i^2 + \sum_{i<k=1}^{N-2} (2\hat{j}_{iz}\hat{j}_{kz} + \hat{j}_{i+}\hat{j}_{k-} + \hat{j}_{i-}\hat{j}_{k+}), \tag{16}$$

where $\hat{j}_i$, $\hat{j}_{iz}$ and $\hat{j}_{i\pm}$ are the angular momentum, its z projection and the ladder operators in the BF frame, respectively.[56] One should notice that $\hat{T}_Q^{(i)}(\mathbf{Q})$ are R-independent. Namely, $\hat{T}_Q$ only parametrically depends on $\mathbf{R}$ through pre-factors without any crossed partial derivative terms between the two coordinate groups.

We have derived the rotational kinetic energy operators in Eq. (10) as

$$\begin{aligned}\hat{T}_{r,CS}^D &= f_{N-1}(\hat{J}^2 - 2\hat{J}_z^2) + (f_{N-2} + f_{N-1})\frac{\hat{J}_z^2}{\sin^2\theta_{N-2}} - 2f_{N-1}\hat{J}_z\hat{l}_0^{BF} \\ &\quad -2f_{N-2}\frac{\hat{J}_z\hat{l}_z^{BF}}{\sin^2\theta_{N-2}},\end{aligned} \tag{17}$$

$$\hat{T}_{r,CS}^C = -f_{N-1}\{(\hat{J}_+\hat{l}_-^{BF} + \hat{J}_-\hat{l}_+^{BF}) - [\hat{J}_+(\hat{J}_z - \frac{1}{2}) + \hat{J}_-(\hat{J}_z + \frac{1}{2})]\cot\theta_{N-2}\}, \tag{18}$$

where $\hat{J}$, $\hat{J}_z$ and $\hat{J}_\pm$ are the total angular momentum, its z component and ladder operators, respectively. They obey the anomalous commutation rules. The other angular operators are determined by the BF angular operators. They are obtained as

$$\hat{l}_z^{BF} = \sum_{k=1}^{N-3} \hat{j}_{kz}, \tag{19}$$

$$\hat{l}_0^{BF} = \sum_{k=1}^{N-3} \{\frac{1}{2}(\hat{j}_{k+} + \hat{j}_{k-}) + \cot\theta_{N-2}\hat{j}_{kz}\} \cot\theta_{N-2}, \tag{20}$$

$$\hat{l}_\pm^{BF} = \sum_{k=1}^{N-3} (\hat{j}_{k\pm} + \cot\theta_{N-2}\hat{j}_{kz}) \pm \hbar\hat{p}_{\theta_{N-2}}, \tag{21}$$

with the operator[57]

$$\hat{p}_\theta = \frac{\partial}{\partial\theta} + \frac{1}{2}\cot\theta. \tag{22}$$

It is worth mentioning that the $\hat{p}_\theta$ matrix in a basis set should be accurately evaluated using either an analytical recurrence[58] or a Gauss-Jacobi quadrature method[57] in order to keep its anti-hermiticity. In Eq. (18), the first term on the right side is the Coriolis coupling. The second one arises from the constraint of vector $\mathbf{r}_{N-2}$ in the xz-plane.

The rovibrational Hamiltonian is general for any polyatomic molecules if the orthogonal polyspherical vectors are defined as in Fig. 1. For a small/medium size molecule ($N \leq 5$), the Hamiltonian can be represented in a set of finite basis representation (FBR) basis set. For instance, if one employs the orthonormal spherical harmonic basis functions $|jm>$, i.e.,[56]

$$< \theta\varphi|jm >= \Theta_j^m(\theta)\frac{1}{\sqrt{2\pi}}e^{im\varphi}, \tag{23}$$

where $\Theta_j^m(\theta)$ are the normalized associated Legendre polynomials, the resulting Hamiltonian matrix is very sparse. Because these functions are the common eigenstates of both $\hat{j}^2$ and $\hat{j}_z$, namely,

$$\hat{j}^2|jm> = j(j+1)\hbar^2|jm>, \tag{24}$$

$$\hat{j}_z|jm> = m\hbar|jm> . \tag{25}$$

For the ladder operators, we have the relationship,

$$\hat{j}_{\pm}|jm>= T^{\pm}_{jm}\hbar|jm\pm 1>,\ T^{\pm}_{jm}=[j(j+1)-m(m\pm 1)]^{1/2}. \tag{26}$$

Generally, an iterative diagonalization method is used, which requires only the action of the Hamiltonian on basis functions. In this circumstance, for the internal angular coordinates, the $\hat{T}_Q-$ and $\hat{T}^{D,C}_{r,CS}-$FBR basis products can be easily computed on-the-fly by using Eqs. (24)-(26).

However, for larger polyatomic molecules, the resulting FBR basis set is too huge to be dealt with. Currently, there is no good way to contract a non-direct product FBR basis. In order to overcome this critical bottleneck, we will explore the discrete variable representation (DVR) method[34,59–66] or its basis contraction scheme in this work. This is also largely motivated by the characters of potential energy surface of system of interest. In the variational approach using a non-direct product FBR basis set, dynamic calculations required access of the whole configuration space, which is not available for the potential energy surfaces of most large polyatomic systems. Nowadays, with the help of modern quantum chemistry calculations, accurate ab initio potential energy surfaces can be obtained for polyatomic systems with up to seven atoms. Those surfaces are normally fitted using an advanced interpolation technology such as the Shepard interpolation,[67] neural network approach,[68] high-order polynomial expansion scheme,[69] and high-dimensional model representation (HDMR) methods.[70–72] Generally speaking, those methods usually give a semi-global potential energy surface that is lack of the extrapolation reliability.

In order to do calculations in DVR, by using the definition of the angular operators in Eqs. (5) and (6), we have obtained the $Q-$dependent kinetic energy operators in coordinate space as follows

$$\begin{aligned}\hat{T}_Q &= \sum_{i=1}^{N-2}(f_i+f_{N-1})\hat{T}_{\theta_i} \\ &\quad + \sum_{j=1}^{N-3}\{\frac{1}{\sin^2\theta_j}f_j+\frac{1}{\sin^2\theta_{N-2}}f_{N-2}+(\cot^2\theta_j+\cot^2\theta_{N-2})f_{N-1}\}\hat{T}_{\varphi_j}\end{aligned}$$

$$
\begin{aligned}
&-2\hbar^2(\frac{1}{\sin^2\theta_{N-2}}f_{N-2}+\cot^2\theta_{N-1}f_{N-1})\sum_{i<j=1}^{N-3}\hat{p}_{\varphi_i}\hat{p}_{\varphi_j}\\
&+2\hbar^2 f_{N-1}\Bigg\{-\sum_{k=1}^{N-4}\cos(\varphi_k-\varphi_{N-3})\hat{p}_{\theta_k}\hat{p}_{\theta_{N-3}}-\sum_{j=1}^{N-3}\cos\varphi_j\hat{p}_{\theta_j}\hat{p}_{\theta_{N-2}}\\
&+\sum_{i\neq j=1}^{N-3}\cot\theta_j\hat{p}_{\theta_j}(\cos\varphi_i\hat{p}^S_{\varphi_j}-\sin\varphi_i\hat{p}^A_{\varphi_j})\\
&+\cot\theta_{N-2}\sum_{j=1}^{N-3}\hat{p}_{\theta_j}[\hat{p}^S_{\varphi_j}+\sin\varphi_j(\sum_{i\neq j=1}^{N-3}\hat{p}_{\varphi_i})]\\
&-\sum_{i<j=1}^{N-3}\cot\theta_i\cot\theta_j(\hat{p}^A_{\varphi_i}\hat{p}^A_{\varphi_j}+\hat{p}^S_{\varphi_i}\hat{p}^S_{\varphi_j})\\
&+\cot\theta_{N-2}\sum_{j=1}^{N-3}\cot\theta_j[\hat{p}^{CS}_{\varphi_j\varphi_j}+\hat{p}^A_{\varphi_j}(\sum_{i\neq j=1}^{N-3}\hat{p}_{\varphi_i})]\\
&+\sum_{j=1}^{N-3}(\cot\theta_j\hat{p}_{\theta_{N-2}}\hat{p}^S_{\varphi_j})\Bigg\},
\end{aligned}
\tag{27}
$$

$$
\hat{l}^{BF}_z=-i\hbar\sum_{k=1}^{N-3}\hat{p}_{\varphi_k},
\tag{28}
$$

$$
\hat{l}^{BF}_0=i\hbar\sum_{k=1}^{N-3}\{\cot\theta_k\hat{p}^A_{\varphi_k}+\sin\varphi_k\hat{p}_{\theta_k}-\cot\theta_{N-2}\hat{p}_{\varphi_k}\}\cot\theta_{N-2},
\tag{29}
$$

$$
\hat{l}^{BF}_{\pm}=\sum_{k=1}^{N-3}\{\pm\hbar e^{\pm i\varphi_k}\hat{p}_{\theta_k}-i\hbar\cot\theta_{N-2}\hat{p}_{\varphi_k}+i\hbar\cot\theta_k\hat{p}^A_{\varphi_k}\mp\hbar\cot\theta_k\hat{p}^S_{\varphi_k}\}\pm\hbar\hat{p}_{\theta_{N-2}},
\tag{30}
$$

with[57]

$$
\hat{T}_\theta = -\frac{\hbar^2}{\sin\theta}\frac{\partial}{\partial\theta}\sin\theta\frac{\partial}{\partial\theta},
\tag{31}
$$

$$
\hat{T}_\varphi = -\hbar^2\frac{\partial^2}{\partial\varphi^2},
\tag{32}
$$

$$
\hat{p}_\varphi = \frac{\partial}{\partial\varphi},
\tag{33}
$$

$$
\hat{p}^A_\varphi = \cos\varphi\frac{\partial}{\partial\varphi}-\frac{1}{2}\sin\varphi,
\tag{34}
$$

$$
\hat{p}^S_\varphi = \sin\varphi\frac{\partial}{\partial\varphi}+\frac{1}{2}\cos\varphi,
\tag{35}
$$

$$
\hat{p}^{CS}_{\varphi\varphi} = \cos\varphi\frac{\partial^2}{\partial\varphi^2}-\sin\varphi\frac{\partial}{\partial\varphi}-\frac{1}{4}\cos\varphi.
\tag{36}
$$

They are general expressions regardless of molecular size. Actually, we have written the rovibrational Hamiltonian in a partitioned structure. And the Hamiltonian is explicitly

Hermitian. For instance, we have the relationships $\hat{T}_Q^\dagger = \hat{T}_Q$ in Eq. (27) and $\hat{l}_-^{BF} = \hat{l}_+^{BF\dagger}$ in Eq. (30). The Hamiltonian is very compact and highly factorized with the highest rank of two. All those properties of Hamiltonian provide an advantage to efficiently calculate the eigenvalues of the system.

Importantly, it was found that the rotation-related kinetic energy operators $\hat{T}_{r,CS}^{D,C}$ (see Eqs. (17) and (18)) depend on the radial coordinates only parametrically. In other words, the rotational couplings are mainly determined in the angular variables via the four operators $\hat{l}_z^{BF}$, $\hat{l}_0^{BF}$, and $\hat{l}_\pm^{BF}$. These four operators are only defined by the vibrational motions in the internal coordinates in the BF frame. Based on this fact, we will use the main results in Eqs. (27)-(30) to develop an efficient iterative diagonalization algorithm for computing the rovibrational states as discussed below.

2.2 Multi-layer Lanczos iterative diagonalization algorithm

The multi-layer Lanczos algorithm[16,35,73] will be extended to solve the rovibrational eigenvalue problem of the molecular Hamiltonian. Since the algorithm has been well described for vibrational spectrum calculations in the literature,[5,7,15,16,35,73] here, we will mainly focus on the discussion of the outer layer Lanczos iteration. The inner nested Lanczos iteration remains the same as in the vibrational calculations. Briefly, the inner layer iteration is used to obtain a set of vibrationally diabatic basis functions $\{|Q_m>\}$ in the internal angular variables $\mathbf{Q}$. They are formed by the lowest eigenstates of a reference Hamiltonian $\hat{H}_Q^0(Q;\mathbf{R}_0,\mathbf{R}_0^V)$, i.e.

$$\hat{H}_Q^0(\mathbf{Q};\mathbf{R}_0,\mathbf{R}_0^V)|Q_m(\mathbf{Q};\mathbf{R}_0,\mathbf{R}_0^V)>=\mathcal{E}_m^0|Q_m(\mathbf{Q};\mathbf{R}_0,\mathbf{R}_0^V)>, \tag{37}$$

with

$$\hat{H}_Q^0(\mathbf{Q};\mathbf{R}_0,\mathbf{R}_0^V)=\hat{T}_Q(\mathbf{Q};\mathbf{R}_0)+V(\mathbf{Q};\mathbf{R}_0^V), \tag{38}$$

where $\mathbf{R}_0$ are the radial references in the kinetic energy operator. Usually, they are constant as $\{r_{i0}\}$. $\mathbf{R}_0^V$ are the references in the potential energy surface, and may be dependent of $\mathbf{R}$

for a better reference potential.[74] In this work, the eigenvalue problem in Eq. (37) is solved by using the neural network iterative diagonalization method (NNiDM)[73] in either DVR or FBR. No more detail will be given. The reader can refer to Refs. [5, 73] and references therein.

The multi-layer Lanczos iterative diagonalization method uses the same approach as the two-layer Lancozs method.[35] The vibrational Hamiltonian has been re-organized as

$$\hat{H}_v = \hat{T}_R(\mathbf{R}) + \hat{H}_Q^0(\mathbf{Q};\mathbf{R}) + \Delta\hat{H}_Q,\ \Delta\hat{H}_Q = \hat{H}_Q(\mathbf{Q};\mathbf{R}) - \hat{H}_Q^0(\mathbf{Q};\mathbf{R}_0,\mathbf{R}_0^V). \tag{39}$$

Once the diabatic functions have been computed, the potential residual matrix $< Q_n|\Delta V(\mathbf{Q};\mathbf{R}_\alpha)|Q_m >$ and the kinetic energy operator matrices $< Q_n|\hat{T}_Q^{(i)}|Q_m >$ are then calculated. The latter are $R-$independent. They are used to construct the $\Delta H_Q(\mathbf{R})$ matrices for the outer layer Lanczos iteration. In order to study the rovibrational states, we will calculate and save six extra small matrices in the diabatic basis functions. They are given by

$$\mathbf{T}_{nm}^Q = < Q_n|\cot\theta_{N-2}|Q_m >, \tag{40}$$

$$\mathbf{S}_{nm}^Q = < Q_n|\frac{1}{\sin^2\theta_{N-2}}|Q_m >, \tag{41}$$

$$\mathbf{D}_{nm}^Q = < Q_n| - 2i\hat{l}_0^{BF}|Q_m >, \tag{42}$$

$$\mathbf{F}_{nm}^Q = < Q_n|\frac{-2i\hat{l}_z^{BF}}{\sin^2\theta_{N-2}}|Q_m >, \tag{43}$$

and

$$\mathbf{A}_{nm}^Q + i\mathbf{B}_{nm}^Q =< Q_n|\hat{l}_+^{BF}|Q_m > . \tag{44}$$

Here $\mathbf{S}^Q$ and $\mathbf{T}^Q$ are real symmetric whereas $\mathbf{A}^Q$, $\mathbf{B}^Q$, $\mathbf{D}^Q$, and $\mathbf{F}^Q$ are real anti-Hermitian. All quantities required have been obtained in the diabatic basis function calculations. Those matrices are calculated only once as they are similar to the ΔV and $\hat{T}_Q^{(i)}$ matrices.

The total Hamiltonian is represented in a direct product basis set in three coordinate groups, $\mathbf{R}$, $\mathbf{Q}$ and overall rotation angles. Such a basis function is written as

$$|\mathbf{R}_\alpha Q_m \Omega >= |\mathbf{R}_\alpha > |Q_m(\mathbf{Q};\mathbf{R}_0,\mathbf{R}_0^V) > |\Omega; JM > \tag{45}$$

with

$$|\Omega; JM >= \frac{1}{\sqrt{2\pi}} e^{i\Omega\phi_{N-2}} |JM\Omega > . \tag{46}$$

Here, $|JM\Omega >$ is a rotational basis function. It is given by the Wigner rotation matrix via the Euler angles[75]

$$< \alpha', \beta', \gamma' | JM\Omega >= \sqrt{\frac{2J+1}{8\pi^2}} D^{J*}_{\Omega M}(\alpha', \beta', \gamma'), \tag{47}$$

where M and Ω are the projections of $\hat{J}$ onto the SF and the BF z-axes, respectively. Without external fields, J and M are good quantum numbers while Ω is a good quantum number only within the coupled state (CS) representation. That is, $|JM\Omega >$ are the eigenstates of both $\hat{J}$ and $\hat{J}_z$. The term $e^{i\Omega\phi_{N-2}}$ in Eq. (46) is used to take the phase factor into account due to the use of direct product basis functions in the angular variables. In practice, the ϕ_{N-2} angle will be set to be the Euler angle γ'. That is, we have $\phi_{N-2} = 0$ and include a vector potential $\mp i/2$ in Eq. (30). In addition, $|\mathbf{R}_\alpha >= \Pi_{i=1}^{N-1} |r_{\alpha_i} >$ refer to the direct-product PO-DVR (potential optimized-discrete variable representation) basis functions in $\mathbf{R}$ with α being a collective DVR index. The 1D PO-DVRs are calculated using the lowest eigenstates of the Hamiltonian $\hat{h}(r)$ in Eq. (12). The direct-product basis functions are further contracted by discarding those PO-DVRs where the minimum potential energies in their corresponding $\mathbf{R}_\alpha$ sectors are larger than a threshold value (V_{th}).

This uncoupled basis set has the orthonormality condition

$$< \mathbf{R}_\alpha | \mathbf{R}_\beta >< Q_n(\mathbf{Q}; \mathbf{R}_0, \mathbf{R}_0^V) | Q_m(\mathbf{Q}; \mathbf{R}_0, \mathbf{R}_0^V) >< \Omega'; JM | \Omega; JM >= \delta_{\alpha\beta} \delta_{nm} \delta_{\Omega'\Omega} \tag{48}$$

that gives a very sparse matrix representation of $\hat{H}$. In the $|\Omega; JM >$ basis expansion, the Hamiltonian matrix is block tri-diagonal. $< \Omega' | \hat{H}_v | \Omega >$ and $< \Omega' | \hat{T}^D_{r,CS} | \Omega >$ appear in the diagonal blocks. The off-diagonal blocks are given by $< \Omega' | \hat{T}^C_{r,CS} | \Omega >$. Indeed, $\hat{H}_v$ is invariant under the overall rotations. For a given total angular momentum J, the explicit matrices for $\hat{T}^{D,C}_{r,CS}$ are

$$< Q_n \Omega' | \hat{T}^D_{r,CS}(\mathbf{R}; J) | Q_m \Omega > \;=\; \Big\{ f_{N-1}[(J(J+1) - 2\Omega^2]\hbar^2 + (f_{N-2} + f_{N-1}) \mathbf{S}^Q_{nm} \Omega^2 \hbar^2$$

$$-if_{N-1}\mathbf{D}^Q_{nm}\Omega\hbar - if_{N-2}\mathbf{F}^Q_{nm}\Omega\hbar\Big\}\,\delta_{\Omega'\Omega}, \tag{49}$$

$$\begin{aligned} < Q_n\Omega'|\hat{T}^C_{r,CS}(\mathbf{R};J)|Q_m\Omega > \;=\; & -f_{N-1}T^+_{J\Omega}[\mathbf{A}^Q_{nm} - \mathbf{T}^Q_{nm}(\Omega+\frac{1}{2})\hbar]\hbar\delta_{\Omega',\Omega+1} \\ & -if_{N-1}T^+_{J\Omega}\mathbf{B}^Q_{nm}\hbar\delta_{\Omega',\Omega\pm1} \\ & -f_{N-1}T^+_{J\Omega}[-\mathbf{A}^Q_{nm} - \mathbf{T}^Q_{nm}(\Omega+\frac{1}{2})\hbar]\hbar\delta_{\Omega',\Omega-1}, \end{aligned} \tag{50}$$

with

$$T^+_{J\Omega} = \sqrt{J(J+1) - \Omega(\Omega+1)}. \tag{51}$$

Here, we have used the relationship $T^-_{J(\Omega+1)} = T^+_{J\Omega}$. The rotational operators $\hat{T}^{D,C}_{r,CS}$ are diagonal in the radial DVR basis $|\mathbf{R}_\alpha>$.

Although the Hamiltonian matrix is very sparse in this basis set, it is complex Hermitian. The complex representation may be not numerically efficient. In order to use a real algorithm, we can utilize more sophisticated rotational basis functions such as the orthonormal Wang functions[41,76] and the signed real rotational functions.[52] Even the universal inversion symmetry can be considered. However, it was found that those advanced treatments will more or less degrade the sparseness of Hamiltonian matrix. For instance, the $(\Omega, \Omega \pm 2)$ blocks occur, which will slow down an iterative diagonalization algorithm. Therefore, in this work, we prefer the complex sparse Hamiltonian matrix but use a real two-component algorithm proposed below. From the numerical point of view, the real two-component algorithm is as nearly efficient as other real methods[41,52] owing to the compensation by the use of sparse matrix. Nevertheless, the two-component method requires twice the core memory, which is not an issue in the multi-layer Lanczos algorithm, especially for a low J because the memory requirement of the algorithm is determined in the vibrationally diabatic function calculations in Eq. (37). The core memory is released after the coupling matrices have been calculated.

Since the complex Hamiltonian matrix is Hermitian, the rovibrational eigenstates can

be calculated using the real standard Lanczos algorithm,[77]

$$\beta_{l+1}|v_{l+1}>=\hat{H}|v_l>-\alpha_l|v_l>-\beta_l|v_{l-1}> \tag{52}$$

with a minor modification. That is, the Lanczos vectors are expressed in a real two-component form. One component represents the real coefficient part (denoted as 'r') of a vector in the basis set while the second component stands for the imaginary part (denoted as 'i'). Therefore, by using the basis set in Eq. (45), the Lanczos vector $|v_l>$ can be expressed as

$$|v_l>=\sum_{t,m,\alpha,\Omega} C^l_{t,m,\alpha,\Omega}|t\mathbf{R}_\alpha Q_m\Omega>,\ t=r,i. \tag{53}$$

The reccurrence coefficients are calculated as usual, namely

$$\alpha_l = <v_l|\hat{H}|v_l>, \tag{54}$$

$$\beta_{l+1} = <v_{j+1}|\hat{H}|v_l> \tag{55}$$

that define a real symmetric tri-diagonal matrix. Diagonalizing the matrix gives the rovibrational eigenstates if converged.

The Lanczos method has been widely used in quantum scattering dynamics calculations with a complex Hamiltonian. Two powerful variants are the short time step Lanczos propagator[78] and the complex Lanczos algorithm for resonance calculations.[79] Usually, those algorithms have the equalivalent of four times real operations in each action of Hamiltonian on vector. In contrast, the real two-component Lanczos method costs about two times the real operations. Furthermore, this algorithm still uses the Herimitian nomalization of Lanczos vectors, compared to the complex normalization condition commonly used in the complex Lanczos method for studying the resonances.[79]

As a typical iterative diagonalization method, the algorithm requires only the action of Hamiltonian on a vector without explicitly storing the whole matrix elements. Here, the crucial $\hat{H}-$vector product can be calculated as

$$\hat{H}|v_l> = \sum_{t',n,\beta,\Omega'}\sum_{t,m,\alpha,\Omega}\Big\{<\mathbf{R}_\beta|\hat{T}_R(\mathbf{R})|\mathbf{R}_\alpha>\delta_{t't}\delta_{nm}\delta_{\Omega'\Omega}+\mathcal{E}^0_m\delta_{t't}\delta_{nm}\delta_{\beta\alpha}\delta_{\Omega'\Omega}+$$

$$< Q_n|\Delta\hat{H}_Q(\mathbf{R}_\alpha)|Q_m > \delta_{t't}\delta_{\beta\alpha}\delta_{\Omega'\Omega} + [\mathbf{T}^{D,J,r}_{n\Omega',m\Omega}(\mathbf{R}_\alpha)\delta_{t't} +$$

$$\mathbf{T}^{D,J,i}_{n\Omega',m\Omega}(\mathbf{R}_\alpha)(\delta_{t'i}\delta_{tr} - \delta_{t'r}\delta_{ti})]\delta_{\beta\alpha}\delta_{\Omega'\Omega} + [\mathbf{T}^{C,J,r}_{n\Omega',m\Omega}(\mathbf{R}_\alpha)\delta_{t't} +$$

$$\mathbf{T}^{C,J,i}_{n\Omega',m\Omega}(\mathbf{R}_\alpha)(\delta_{t'i}\delta_{tr} - \delta_{t'r}\delta_{ti})]\delta_{\beta\alpha}\delta_{\Omega'\Omega\pm1}\Big\} C^l_{t,m,\alpha,\Omega}|t'\mathbf{R}_\beta Q_n\Omega' > \tag{56}$$

with

$$< \mathbf{R}_\beta|\hat{T}_R(\mathbf{R})|\mathbf{R}_\alpha >= \sum_{i=1}^{N-1}\Big\{< r_{\beta_i}|\hat{h}_{r_i}(r_i)|r_{\alpha_i} > -V_0(\mathbf{R}_{\alpha_i})\delta_{\beta_i\alpha_i}\Big\}\Pi_{j\neq i}\delta_{\beta_j\alpha_j}. \tag{57}$$

Here, $\mathbf{T}^{D,J,r}_{n\Omega',m\Omega}(\mathbf{R}_\alpha)$ and $\mathbf{T}^{D,J,i}_{n\Omega',m\Omega}(\mathbf{R}_\alpha)$ are the real and imaginary part of the quantity $< Q_n\Omega'|\hat{T}^D_{r,CS}(\mathbf{R};J)|Q_m\Omega >$ in Eq. (49) at the DVR point $|\mathbf{R}_\alpha >$ for a given J. Similarly, $\mathbf{T}^{C,J,r}_{n\Omega',m\Omega}(\mathbf{R}_\alpha)$ and $\mathbf{T}^{C,J,i}_{n\Omega',m\Omega}(\mathbf{R}_\alpha)$ are the real and imaginary part of $< Q_n\Omega'|\hat{T}^C_{r,CS}(\mathbf{R};J)|Q_m\Omega >$ in Eq. (50). As a result, all calculations are performed in real.

Roughly, the basis size used in Eq. (56) is about or less than $2(2J+1)N_RN_Q^{diab}$ for a given J, where N_R and N_Q^{diab} are the primitive PODVR basis size in $\mathbf{R}$ and the number of diabatic basis functions in $\mathbf{Q}$. $(2J+1)$ counts for the summation of Ω from $-J$ to J. The basis size is often much smaller than that in the original full dimensional representation. This salient feature is attributed to the multi-layer Lanczos iteration approach. In addition, the resulting Hamiltonian matrix as seen in Eq. (56) is very sparse so that the eigenstates can be efficiently solved by an iterative diagonalization method. Compared to the pure vibrational state calculations, the rovibrational state calculations require only six extra small matrices (see Eqs. (40)-(44)). The computational efforts are proportional to $2(2J+1)$ in the outer layer Lanczos iteration. Furthermore, the calculations for different J are completely independent, which is very suitable for parallel computing. Importantly, the expensive computational steps (the calculations of diabatic basis functions and residual potential energy terms) remain unchanged as used in vibrational calculations.

In particular, this proposed algorithm is a rigorous quantum dynamics method without any dynamics approximation. It is problem-independent so that the algorithm can be used for studying varieties of polyatomic molecular systems through selecting the combination of $(N-1)$ orthogonal polyspherical vectors. In the next section, we will demonstrate two

realistic examples.

3 Applications

In this section, we will discuss two applications of the algorithm for computing the rovibrational energy levels of CH_4 and H_2CO using the same program. In order to compare the calculated results, the SPT8 potential energy surface[39] of CH_4 will be used for the methane study although there are other accurate surfaces available.[80–84] In particular, some benchmark calculations on the rovibrational energy levels of CH_4 were reported using the SPT8 surface.

3.1 CH_4

For penta-atomic molecules, there are 21 sets of orthogonal polyspherical coordinates in the PetroVib program.[15] In this study, the (4+1) Radau coordinates (labeled as Icd=2) is employed. It is an optimal choice for methane, and has been widely used by other groups.[16,39,84] In the calculations, the rovibrational Hamiltonian is represented in a full DVR approach. Ten PO-DVR functions are used for each radial coordinate, which gives a basis size of $N_R = 10$K. For the polar angles, 31 associated Legendre (with $m = 1$) or Legendre DVR points are utilized in each degree-of-freedom. 61 Fourier DVR functions are employed for each azimuthal angle. The DVR basis set is contracted by using a potential threshold value of $V_{th} = 3.25\,\mathrm{eV}$. The final DVR basis size in the internal angular variables is obtained as $N_Q = 1644877$ (or $N_Q = 1513985$ for the Legendre DVRs). 380 (N_Q^{diab}) vibrationally diabatic functions are calculated using the neural network iterative diagonalization method.[73] The reference radial coordinates in the kinetic energy operators are $2.05241\,\mathrm{a}_0$ for r_{i0}, with its associated mass $\mu_i = 1.007825035\,\mathrm{amu}$ relative to $m_\mathrm{C} = 12.0\,\mathrm{amu}$. Those parameters can well converge the rovibrational energies up to 6000 cm^{-1}. Since the results obtained with the Legendre DVR basis are essentially the same as those

with the associated Legendre DVRs, only the latter's results are reported here.

Table 1 lists the calculated energy levels of CH_4 together with a comparison with experimental and previous theoretical results,[36,85] where the energy levels are labeled as "$(v_1v_3)(v_2v_4)$symmetry" following the polyads. We used the same level symmetries as previous works.[14,36,86] $v_1(A_1)$ and $v_3(F_2)$ are the stretching modes of CH_4 while $v_2(E)$ and $v_4(F_2)$ are the bending ones. Compared to the theoretical results,[36] they are in excellent agreement for both vibrational and rovibrational energy levels up to highly excited states. Our results are slightly lower than the contracted Lanczos calculations of Wang and Carrington. However, the differences are small. It gives a root-mean-square deviation of 0.05 cm^{-1}. The smaller values are due to the fact that a DVR approach is not variational. It was also noticed that the full DVR respresentation of Hamiltonian slightly slows down the convergence of energy levels with respect to the basis size, especially in the angular coordinates. The spectral range of the angular kinetic energy operator is larger in DVR than in FBR. Importantly, it does not affect the accurate calculation of rovibrational energy levels. As expected, compared to the experimental values, the errors are large in some rovibrational states. This is due to the accuracy of the potential energy surface. Most recently, Wang and Carrington[84] have adjusted this surface according to the experimental values and the refined surface is very accurate.

All calculations require about 13.6GB core memory, 18GB disk space and 420 hours CPU time on a CRAY XC40 supercomputer. The CPU time is mainly spent in calculating the diabatic functions (55.2%) and the potential energies on grids for the construction of the potential residual ΔV (39.8%). Of course, the latter strongly depends on the complexity of the surface used. For the outer layer Lanczos iterations, it took only a few hours CPU time to calculate the rovibrational eigenstates, and demanded less than 3GB core memory. For instance, it cost (in hours) about 0.6, 3.8, 8.7 and 16.1 to carry out 5000 Lanczos iterations for $J = 0$, 1, 2, and 3, respectively. This shows a nearly linear

scaling as J (≥ 1). Since only real one-component operations are needed for $J = 0$, the CPU time has a big increase for $J = 1$ upon the onset of the $2(2J + 1)$ factor. This numerical example demonstrates that the new algorithm is highly accurate and efficient for computing rovibrational states of polyatomic molecules.

3.2 H_2CO

In this example, we will demonstrate that the theory described in Sec. 2 is general. That is, it can be used for any polyatomic system. Basically, we treat the H_2CO molecule as a pseudo five-atomic molecule H_2GCO so that its rovibrational states can be studied using the same program as for CH_4 discussed above. Here, we used the (3+1) Radau and Jacobi coordinates (i.e. the Icd=3 set in the PetroVib code),[15] which is shown in Fig. 2. The $\mathbf{r}_2$ Radau vector is associated with the dummy atom G with a zero mass. In this application, we need only to set $\mu_2 = 0$, $f_2(r_2) = 0$ in Eq. (14), the associated basis sizes $(N_{r_2}, N_{\theta_2}, N_{\varphi_2})$ being one, and the 1D kinetic energy operator matrices in Eqs. (22) and (31)-(36) being zero. This treatment is equivalent to removing one vector. The calculations are performed on the ab initio quartic force field of Burleigh et al.[87]

Similar to the calculations of CH_4, a full DVR representation is employed. Nine PO-DVR functions are used for each C-H stretching coordinate while 11 PODVRs are for the O-CH_2 Jacobi radial variable. The basis size in the radial coordinates is 891. 35 associated Legendre (with $m = 1$) DVRs are used in each polar angle; and 69 Fourier DVR functions are for the azimuthal coordinate. The potential threshold value used is $V_{th} = 3.0\,\mathrm{eV}$ that determines a contracted basis size of 7870 in $\mathbf{Q}$. 150 vibrationally diabatic functions are used. The reference radial coordinates in the kinetic energy operators are $2.042629\,\mathrm{a}_0$ for $r_{1,0}$ and $r_{3,0}$, and $2.44428\,\mathrm{a}_0$ for $r_{4,0}$. The atomic masses are 1.007825035 amu for H, 12.0 amu for C, and 15.994915 amu for O.

Table 2 gives the calculated energy levels of H_2CO together with a comparison with previous calculations.[51,87] As one can see, they are in excellent agreement. The whole

calculations took less than one hour although it is not the best way to do so in such a reduced dimension way. Importantly, this application justifies that the algorithm is universal for general polyatomic molecules.

4 Conclusion

We have developed a novel exact variational algorithm for calculating rovibrational energies of polyatomic molecules for a given potential energy surface. An explicitly Hermitian Hamiltonian for an $N-$body system has been derived using a set of orthogonal spherical coordinates in the body-fixed frame. The rovibrational Hamiltonian has a universal formulation regardless of the choice of orthogonal polyspherical coordinates and the number of atoms in molecule, which is suitable for developing a general program to study the rovibrational spectra of many polyatomic systems. The large amplitude motion of vibrations is naturally described in the curvilinear coordinates.

By using the partitioned structure of the Hamiltonian and the coupled-state scheme, the multi-layer Lanczos method has been extended to solve the eigenvalue problem of the system in a group direct product basis set. A real two-component Lanczos algorithm is also proposed for solving the energy levels of the resulting complex Hermitian matrix. Compared to the pure vibrational state calculations, the rovibrational state calculations requires only a few extra small matrices that are independent of the overall rotational variables and radial coordinates. For a given total angular momentum J, the rovibrational states can be efficiently computed via a Lanczos iterative diagonalization method. In particular, the algorithm is a rigorous full dimensional method without any dynamics approximation while still keeping the merit of the multi-layer Lanczos method, i.e. solving the whole eigenvalue problem in a reduced-dimension manner. Parallel computing can be easily implemented with the algorithm.

The extended multi-layer Lanczos algorithm has been applied to the rovibrational state

calculations of CH_4 and H_2CO. The obtained results are in good agreement with the previous calculations. In this application, we have demonstrated an important point that the rovibrational states of both CH_4 and H_2CO can be calculated using the same program. This feature is similar to those normal mode based methods[1,13,14] but this approach is able to describe the large amplitude motion of vibrations easily. Actually, such an accomplishment is largely attributed by the general formulation of the rovibrational Hamiltonian and by the flexible choice of orthogonal polyspherical coordinates. Although the latter has not been discussed in detail in this work, it has already been demonstrated in previous works.[3,15,42,47] This research also shows that it is practically possible for developing a problem-independent algorithm for the rovibrational spectrum calculations of polyatomic molecules with large amplitude motion. As a result, the tedious programming in dynamics calculations from system to system can be avoided.

Although we used two rigid molecules to demonstrate the algorithm, it is no doubt applicable for studying molecules with LAM. Now, the algorithm is used to study two floppy molecules, the hydroxymethyl (CH_2OH) and vinyl (C_2H_3) radicals. The hydroxymethyl radical has two large amplitude coordinates. Our preliminary calculations are in excellent agreement with the diffusion Monte Carlo results of Harding.[88] In addition, the vinyl radical has one floppy coordinate (the in-plane bending motion of the $\alpha-$CH of C_2H_3). By using the recent ab initio potential energy surface of Chen et al.,[89] we have accuately calculated the lowest hundreds of rovibrational states of C_2H_3. The results will be published elsewhere.

Acknowledgments

This work was performed at Brookhaven National Laboratory under Contract No. DE-SC0012704 with the U.S. Department of Energy, Office of Science, and supported by its Division of Chemical Sciences, Geosciences and Biosciences within the Office of Basic

Energy Sciences. It also used the resource at the National Energy Research Scientific Computing Center (NERSC) under Contract No. DE-AC02-05CH11231.

References

[1] J.M. Bowman, T. Carrington Jr., and H.-D. Meyer, *Mol. Phys.* **106**, 2145 (2008).

[2] H.-D. Meyer, F. Gatti, and G. A. Worth eds, *Multidimensional Quantum Dynamics: MCTDH Theory and Applications* (Wiley-VCH, Weinheim, Germany, 2009).

[3] F. Gatti and C. Iung, *Phys. Rep.* **484**, 1 (2009).

[4] A.G. Csazar, C. Fabri, T. Szidarovsky, E. Matyus, T. Furtenbacher, and G. Czako, *Phys. Chem. Chem. Phys.* **14**, 1085 (2012).

[5] G. Nyman and H.-G. Yu, *Int. Rev. Phys. Chem.* **32**, 39 (2013).

[6] F. Huarte-Larrañaga and U. Manthe, *J. Chem. Phys.* **117**, 4635 (2002).

[7] H.-G. Yu, *J. Chem. Phys.* **120**, 2270 (2004).

[8] X.-G. Wang and T. Carrington Jr., *J. Chem. Phys.* **129**, 234102 (2008).

[9] O. Vendrell, F. Gatti, and H.-D. Meyer, *J. Chem. Phys.* **127**, 184303 (2007).

[10] M. Schroder, F. Gatti, and H.-D. Meyer, *J. Chem. Phys.* **134**, 234307 (2011).

[11] T. Hammer and U. Manthe, *J. Chem. Phys.* **136**, 054105 (2012).

[12] A.V. Nikitin, M. Rey, and V.G. Tyuterev, *J. Chem. Phys.* **142**, 094118 (2015).

[13] J.M. Bowman, S. Carter, and X.C. Huang, *Int. Rev. Phys. Chem.* **22**, 533 (2003).

[14] E. Matyus, J. Simunek, and A.G. Csaszar, *J. Chem. Phys.* **131**, 074106 (2009).

[15] H.-G. Yu, *J. Mol. Spectrosc.* **256**, 287 (2009).

[16] H.-G. Yu, *J. Chem. Phys.* **142**, 044106 (2015).

[17] G.D. Carney, L.L. Sprandel, and C.W. Kern, *Adv. Chem. Phys.* **37**, 305 (1978).

[18] J.M. Bowman, K. Christoffel, and F. Tobin, *J. Phys. Chem.* **83**, 905 (1979).

[19] M. Neff and G. Rauhut, *J. Chem. Phys.* **131**, 124129 (2009).

[20] P. Seidler and O. Christiansen, *J. Chem. Phys.* **131**, 234109 (2009).

[21] J.A. Faucheaux and S. Hirata, *J. Chem. Phys.* **143**, 134105 (2015).

[22] G. Jolicard, *Chem. Phys.* **115**, 57 (1987).

[23] N.C. Handy, *Mol. Phys.* **61**, 207 (1987).

[24] T.J. Lukka, *J. Chem. Phys.* **102**, 3945 (1995).

[25] S. Carter, N.C. Handy, and J. Demaison, *Mol. Phys.* **90**, 729 (1997).

[26] J.H. Frederick and C. Woywod, *J. Chem. Phys.* **111**, 7255 (1999).

[27] D. Luckhaus, *J. Chem. Phys.* **113**, 1329 (2000).

[28] M. Mladenović, *J. Chem. Phys.* **112**, 1070 (2000).

[29] C. Iung and F. Gatti, *Int. J. Quantum Chem.* **106**, 130 (2006).

[30] M. Herman, J. Lievin, J.V. Auwera, and A. Campargue eds., *Advances in Chemical Physics: Global and Accurate Vibration Hamiltonians from High-Resolution Molecular Spectroscopy, Vol.108* (John Wiley & Sons, INC., New York, 1999).

[31] B.T. Sutcliffe, *in Current Aspects of Quantum Chemistry, R. Carbo, ed.* (Elsevier, Amsterdam, 1982).

[32] Z. Bačić and J.C. Light, *Ann. Rev. Phys. Chem.* **40**, 469 (1989).

[33] H. Guo, *Rev. Comput. Chem.* **25**, 285 (2007).

[34] U. Manthe, *J. Chem. Phys.* **130**, 054109 (2009).

[35] H.-G. Yu, *J. Chem. Phys.* **117**, 8190 (2002).

[36] X.-G. Wang and T. Carrington Jr., *J. Chem. Phys.* **121**, 2937 (2004).

[37] A. Leclerc and T. Carrington Jr., *J. Chem. Phys.* **140**, 174111 (2014).

[38] D. Lauvergnat and A. Nauts, *Spectrochimica Acta A* **119**, 18 (2014).

[39] D.W. Schwenke and H. Partridge, *Spectrochimica Acta* **A57**, 887 (2001).

[40] X.-G. Wang and T. Carrington, Jr., *J. Chem. Phys.* **138**, 104106 (2013).

[41] C. Fabri, E. Matyus, T. Furtenbacher, L. Nemes, B. Mihaly, T. Zoltani, and A. Csaszar, *J. Chem. Phys.* **135**, 094307 (2011).

[42] M.J. Bramley and T. Carrington Jr., *J. Chem. Phys.* **99**, 8519 (1993).

[43] C. Leforestier, A. Viel, F. Gatti, C. Muñoz, and C. Iung, *J. Chem. Phys.* **114**, 2099 (2001).

[44] R.E. Wyatt and J.Z.H. Zhang eds., *Dynamics of Molecules and Chemical Reactions* (Dekker, New York, 1996).

[45] R. Radau, *Ann. Sci. Ecole Normale Supérior* **5**, 311 (1868).

[46] A.B. McCoy and E.L. Sibert III, *J. Chem. Phys.* **105**, 459 (1996).

[47] H.-G. Yu and J.T. Muckerman, *J. Mol. Spectrosc.* **214**, 11 (2002).

[48] H.-G. Yu, S. Ndengue, J. Li, R. Dawes, and H. Guo, *J. Chem. Phys.* **143**, 084311 (2015).

[49] H.-G. Yu, H. Han, and H. Guo, *J. Phys. Chem. A* **120**, 2185 (2016).

[50] X.-G. Wang and T. Carrington Jr., *J. Chem. Phys.* **117**, 6923 (2002).

[51] H.-G. Yu, *Chem. Phys. Lett.* **365**, 189 (2002); Erratum **367**, 791 (2003).

[52] A.V. Marenich and J.E. Boggs, *J. Chem. Phys.* **119**, 10105 (2003).

[53] R. Wodraszka and U. Manthe, *J. Phys. Chem. A* **117**, 7246 (2013).

[54] X. Chapuisat and C. Iung, *Phys. Rev.* **A45**, 6217 (1992).

[55] F. Gatti, C. Iung, M. Menou, Y. Justum, A. Nauts, and X. Chapuisat, *J. Chem. Phys.* **108**, 8804 (1998).

[56] A.R. Edmonds, *Angular Momentum in Quantum Mechanics* (Princeton University Press,, Princeton, NJ, 1960).

[57] H.-G. Yu, *J. Chem. Phys.* **117**, 2030 (2002).

[58] B. Poirier, *Chem. Phys.* **308**, 305 (2005).

[59] J.C. Light and T. Carrington Jr., *Adv. Chem. Phys.* **114**, 263 (2000).

[60] J.C. Light, I.P. Hamilton, and J.V. Lill, *J. Chem. Phys.* **82**, 1400 (1985).

[61] B. Poirier and J.C. Light, *J. Chem. Phys.* **111**, 4869 (1999).

[62] J. Echave and D.C. Clary, *Chem. Phys. Lett.* **190**, 225 (1992).

[63] H. Wei and T. Carrington, Jr., *J. Chem. Phys.* **97**, 3029 (1992).

[64] D.J. Haxton, *J. Phys. B* **40**, 4443 (2007).

[65] H.-G. Yu, *J. Chem. Phys.* **122**, 164107 (2005).

[66] V. Szalay and P. Adam, *J. Chem. Phys.* **137**, 064118 (2012).

[67] J. Ischtwan and M.A. Collins, *J. Chem. Phys.* **100**, 8080 (1994).

[68] B. Jiang and H. Guo, *J. Chem. Phys.* **139**, 054112 (2013).

[69] B.J. Braams and J.M. Bowman, *Int. Rev. Phys. Chem.* **28**, 577 (2009).

[70] H. Rabitz and O.F. Alis, *J. Math. Chem.* **25**, 197 (1999).

[71] O.F. Alis and H. Rabitz, *J. Math. Chem.* **29**, 127 (2001).

[72] B. Ziegler and G. Rauhut, *J. Chem. Phys.* **144**, 114114 (2016).

[73] H.-G. Yu, *Phys. Chem. Chem. Phys.* **17**, 14071 (2015).

[74] H.-G. Yu, *J. Chem. Phys.* **121**, 6334 (2004).

[75] R.N. Zare, *Angular Momentum* (Wiley, New York, 1988).

[76] S. Carter, N.C. Handy, C. Puzzarini, R. Tarroni, and P. Palmieri, *Mol. Phys.* **98**, 1697 (2000).

[77] C. Lanczos, *J. Res. Nat. Bur. Stand.* **45**, 255 (1950).

[78] T.J. Park and J.C. Light, *J. Chem. Phys.* **85**, 5870 (1986).

[79] N. Moiseyev, *Non-Hermitian Quantum Mechanics*, Cambridge University Press, Cambridge, 2011.

[80] A.V. Nikitin, M. Rey, and V.G. Tyuterev, *Chem. Phys. Lett.* **501**, 179 (2011).

[81] R. Marquard and M. Quack, *J. Phys. Chem. A* **108**, 3166 (2004).

[82] C. Oyanagi, K. Yagi, and T. Taketsugu et al., *J. Chem. Phys.* **124**, 064311 (2006).

[83] S.N. Yurchenko, J. Tennyson, R.J. Barber, and W. Thiel, *J. Mol. Spectrosc.* **291**, 69 (2013).

[84] X.-G. Wang and T. Carrington, Jr., *J. Chem. Phys.* **141**, 154106 (2014).

[85] Ch. Wenger and J.-P. Champion, *J. Quant. Spectrosc.: Radiat. Trans.* **59**, 471 (1998).

[86] S.L. Mielke, A. Chakraborty, and D.G. Truhlar, *J. Phys. Chem. A* **117**, 7327 (2013).

[87] D.C. Burleigh, A.B. McCoy, and E.L. Sibert III, *J. Chem. Phys.* **104**, 480 (1996).

[88] L. Harding, (private communications).

[89] L. Chen, K. Shao, J. Chen, M. Yang, and D. H. Zhang, *J. Chem. Phys.* **144**, 194309 (2016).

Table 1: Comparison of rovibrational energy levels (in cm^{-1}) of CH_4 up to the octad polyad with the previous theoretical and experimental results.[36,85] Calculations are carried out on the SPT8 potential energy surface.[39] Δ_{WC} and Δ_{expt} are the differences between the WC and experimental values and this work. The zero-point energy (ZPE) level is given by the ground state (GS) $(00)(00)A_1$
.

$(v_1v_3)(v_2v_4)$sym	J	this work	WC[36]	Δ_{WC}	Expt.[36,85]	Δ_{expt}
		GS				
$(00)(00)A_1$	0	9691.528	9691.53	0.00	-	-
F_1	1	10.430	10.43	0.00	10.48	0.05
$(00)(01)F_2$	0	1311.724	1311.74	0.02	1310.76	-0.96
A_2	1	1312.394	1312.41	0.02	1311.43	-0.96
F_2	1	1317.234	1317.25	0.02	1316.30	-0.93
F_1	1	1326.713	1326.73	0.02	1325.82	-0.89
E	1	1327.013	1327.03	0.02	1326.13	-0.88
$(00)(10)E$	0	1533.221	1533.24	0.02	1533.33	0.11
F_2	1	1543.771	1543.79	0.02	1543.93	0.16
F_1	1	1543.891	1543.91	0.02	1544.05	0.16
$(00)(02)A_1$	0	2589.739	2589.77	0.03	2587.04	-2.70
F_1	1	2599.989	2600.02	0.03	2597.34	-2.65
F_1	1	2615.578	2615.61	0.03	2613.45	-2.13
$(00)(02)F_2$	0	2616.208	2616.24	0.03	2614.26	-1.95
E	1	2622.018	2622.05	0.03	2620.09	-1.93
F_2	1	2626.608	2626.64	0.03	2624.50	-2.11
$(00)(02)E$	0	2627.258	2627.29	0.03	2624.62	-2.64
A_2	1	2634.797	2634.83	0.03	2632.96	-1.84
F_2	1	2641.547	2641.58	0.03	2639.20	-2.35
F_1	1	2643.997	2644.03	0.03	2641.61	-2.39
$(00)(11)F_2$	0	2831.485	2831.52	0.03	2830.32	-1.17
E	1	2835.765	2835.80	0.03	2834.66	-1.11
F_1	1	2837.815	2837.85	0.04	2836.69	-1.12
F_2	1	2843.495	2843.53	0.04	2842.40	-1.09
$(00)(11)F_1$	0	2846.875	2846.91	0.04	2846.08	-0.79
A_2	1	2848.835	2848.87	0.04	2847.72	-1.11
F_2	1	2856.614	2856.65	0.04	2855.82	-0.79
E	1	2857.985	2858.02	0.04	2857.20	-0.78
F_1	1	2860.355	2860.39	0.04	2859.61	-0.74
A_1	1	2862.305	2862.34	0.04	2861.58	-0.72

$(10)(00)A_1$	0	2913.675	2913.71	0.04	2916.48	2.81
F_1	1	2924.125	2924.16	0.04	2926.99	2.87
$(01)(00)F_2$	0	3013.564	3013.60	0.04	3019.49	5.93
A_2	1	3022.773	3022.81	0.04	3028.75	5.98
F_2	1	3023.324	3023.36	0.04	3029.31	5.99
F_1	1	3024.463	3024.50	0.04	3030.44	5.98
E	1	3024.524	3024.56	0.04	3030.50	5.98
$(00)(20)A_1$	0	3063.443	3063.48	0.04	3063.65	0.21
$(00)(20)E$	0	3064.972	3065.01	0.04	3065.14	0.17
F_1	1	3074.222	3074.26	0.04	3074.47	0.25
F_2	1	3075.762	3075.80	0.04	3075.98	0.22
F_1	1	3075.782	3075.82	0.04	3076.01	0.23
$(00)(03)F_2$	0	3874.693	3874.74	0.05	3870.49	-4.20
A_2	1	3875.905	3875.95	0.04	3871.54	-4.37
F_2	1	3880.494	3880.54	0.05	3876.22	-4.27
F_1	1	3888.892	3888.94	0.05	3884.73	-4.16
E	1	3889.164	3889.22	0.06	3885.02	-4.14
$(00)(03)A_1$	0	3912.215	3912.26	0.04	3909.19	-3.03
F_1	1	3912.533	3912.58	0.05	3909.15	-3.38
E	1	3922.442	3922.49	0.05	3918.30	-4.14
$(00)(03)F_1$	0	3924.032	3924.08	0.05	3920.52	-3.51
A_1	1	3928.442	3928.49	0.05	3924.92	-3.52
F_1	1	3932.712	3932.76	0.05	3928.85	-3.86
F_2	1	3933.031	3933.08	0.05	3929.31	-3.72
$(00)(03)F_2$	0	3935.272	3935.32	0.05	3930.92	-4.35
F_1	1	3946.471	3946.52	0.05	3942.67	-3.80
E	1	3953.200	3953.25	0.05	3949.29	-3.91
F_2	1	3956.680	3956.73	0.05	3952.56	-4.12
A_2	1	3960.161	3960.21	0.05	3955.91	-4.25
$(00)(12)E$	0	4104.390	4104.44	0.05	4104.62	0.23
F_2	1	4114.221	4114.27	0.05	4114.81	0.59
F_1	1	4114.669	4114.72	0.05	4115.15	0.48
F_1	1	4130.199	4130.25	0.05	4127.47	-2.73
$(00)(12)F_1$	0	4131.209	4131.26	0.05	4128.73	-2.48
$(00)(12)A_1$	0	4135.710	4135.76	0.05	4133.02	-2.69
A_1	1	4138.250	4138.30	0.05	4135.52	-2.73
F_2	1	4138.312	4138.36	0.05	4135.75	-2.56
E	1	4140.218	4140.27	0.05	4137.55	-2.67
$(00)(12)F_2$	0	4144.780	4144.83	0.05	4142.86	-1.92
A_2	1	4150.590	4150.64	0.05	4148.40	-2.19
F_1	1	4150.735	4150.77	0.04	4148.22	-2.51
F_2	1	4151.080	4151.13	0.05	4148.76	-2.32

$(00)(12)E$	0	4153.669	4153.72	0.05	4151.00	-2.67
F_1	1	4158.297	4158.35	0.05	4155.80	-2.50
E	1	4160.347	4160.40	0.05	4158.17	-2.18
$(00)(12)A_2$	0	4164.269	4164.32	0.05	4161.91	-2.36
F_2	1	4167.677	4167.73	0.05	4165.12	-2.56
F_1	1	4169.068	4169.12	0.05	4166.64	-2.43
F_2	1	4178.777	4178.83	0.05	4176.37	-2.41
$(10)(01)F_2$	0	4221.789	4221.84	0.05	4223.46	1.67
A_2	1	4222.239	4222.29	0.05	4223.91	1.67
F_2	1	4227.209	4227.26	0.05	4228.90	1.69
F_1	1	4236.918	4236.97	0.05	4238.65	1.73
E	1	4237.189	4237.24	0.05	4238.93	1.74
$(01)(01)F_2$	0	4314.178	4314.23	0.05	4319.21	5.03
F_1	1	4316.778	4316.83	0.05	4321.68	4.90
$(01)(01)E$	0	4317.538	4317.59	0.05	4322.20	4.66
$(01)(01)F_1$	0	4317.778	4317.83	0.05	4322.58	4.80
$(01)(01)A_1$	0	4318.368	4318.42	0.05	4322.69	4.32
E	1	4320.898	4320.95	0.05	4325.96	5.06
F_2	1	4321.968	4322.02	0.05	4326.82	4.85
A_1	1	4322.358	4322.41	0.05	4327.19	4.83
F_1	1	4322.918	4322.97	0.05	4327.60	4.68
A_2	1	4328.628	4328.68	0.05	4333.68	5.05
F_2	1	4330.488	4330.54	0.05	4335.41	4.92
F_1	1	4331.628	4331.68	0.05	4336.30	4.67
E	1	4331.948	4332.00	0.05	4336.83	4.88
F_1	1	4332.427	4332.48	0.05	4337.15	4.72
F_2	1	4332.808	4332.86	0.05	4337.64	4.83
$(00)(21)F_2$	0	4350.017	4350.07	0.05	4348.71	-1.31
A_2	1	4354.913	4354.96	0.05	4353.62	-1.29
F_2	1	4357.260	4357.31	0.05	4356.01	-1.25
E	1	4358.322	4358.37	0.05	4357.00	-1.32
F_1	1	4361.020	4361.07	0.05	4359.75	-1.27
$(00)(21)F_1$	0	4364.657	4364.71	0.05	4363.59	-1.07
F_2	1	4373.079	4373.13	0.05	4371.80	-1.28
E	1	4376.511	4376.56	0.05	4375.19	-1.32
F_1	1	4378.511	4378.56	0.05	4377.20	-1.31
$(00)(21)F_2$	0	4379.677	4379.73	0.05	4378.98	-0.70
A_1	1	4380.161	4380.21	0.05	4378.88	-1.28
A_2	1	4390.141	4390.19	0.05	4389.45	-0.69
F_2	1	4390.511	4390.56	0.05	4389.84	-0.67
F_1	1	4392.131	4392.18	0.05	4391.49	-0.64
E	1	4393.221	4393.27	0.05	4392.54	-0.68

$(10)(10)E$	0	4432.167	4432.22	0.05	4435.12	2.95
F_2	1	4442.786	4442.84	0.05	4456.99	14.20
F_1	1	4443.016	4443.07	0.05	4457.23	14.21
$(01)(10)F_1$	0	4531.315	4531.37	0.05	4537.55	6.23
$(01)(10)F_2$	0	4537.765	4537.82	0.05	4543.76	5.99
E	1	4541.305	4541.36	0.05	4547.62	6.31
F_2	1	4541.415	4541.47	0.05	4547.73	6.31
F_1	1	4542.185	4542.24	0.05	4548.48	6.29
A_1	1	4542.605	4542.66	0.05	4548.90	6.29
F_1	1	4547.735	4547.79	0.05	4553.78	6.04
E	1	4547.935	4547.99	0.05	4553.98	6.04
F_2	1	4548.805	4548.86	0.05	4554.84	6.03
A_2	1	4549.535	4549.59	0.05	4555.56	6.02
$(00)(30)E$	0	4591.864	4591.92	0.06	4592.01	0.15
$(00)(30)A_2$	0	4595.104	4595.16	0.06	4595.28	0.18
$(00)(30)A_1$	0	4595.374	4595.43	0.06	4595.46	0.09
F_2	1	4602.758	4602.81	0.05	4603.01	0.25
F_1	1	4603.090	4603.14	0.05	4603.27	0.18
F_2	1	4606.175	4606.23	0.05	4606.43	0.25
F_1	1	4606.449	4606.50	0.05	4606.50	0.05

Table 2: Comparison of rovibrational energy levels (in cm^{-1}) of H_2CO calculated from the ab initio quartic potential of BMS[87] with the previous results.[51,87]

State	J	this work	BMS[87]	Y[51]
ZPE	0	5774.993		
	1	2.408		
		10.544		
		10.702		
v_4	0	1167.287	1167.3	1167.29
	1	1169.684		1169.68
		1176.479		1176.48
		1176.618		1176.62
v_6	0	1248.859	1248.9	1248.86
	1	1251.264		1251.26
		1260.719		1260.72
		1260.881		1260.88
v_3	0	1499.489	1499.5	1499.49
	1	1501.904		1501.90
		1510.098		1510.10
		1510.268		1510.27
v_2	0	1746.114	1746.1	1746.11
	1	1748.507		1748.51
		1756.646		1756.65
		1756.806		1756.81
$2v_4$	0	2327.845	2327.9	2327.85
	1	2330.232		2330.23
		2336.417		2336.31
		2336.542		2336.55
$v_4 + v_6$	0	2421.953	2422.0	2421.95
	1	2424.344		2424.35
		2430.979		2430.99
		2431.110		2431.12
$2v_6$	0	2494.969	2495.0	2494.97
	1	2497.369		2497.37
		2508.887		2508.90
		2509.049		2509.06
$v_3 + v_4$	0	2665.987	2666.0	2665.98
	1	2668.389		2668.39
		2674.643		2674.65
		2674.782		2674.79

$v_3 + v_6$	0	2718.062	2718.2	2718.06
	1	2720.476		2720.48
		2730.483		2730.51
		2730.652		2730.68
v_1	0	2782.302	2782.3	2782.27
	1	2784.709		2784.68
		2792.684		2792.66
		2792.846		2792.82
v_5	0	2842.460	2842.5	2842.44
	1	2844.862		2844.84
		2852.821		2852.81
		2852.981		2852.97
$v_2 + v_4$	0	2905.883	2905.9	2905.88
	1	2908.266		2908.27
		2915.573		2915.58
		2915.715		2915.72
$2v_3$	0	2998.143	2998.1	2998.16
	1	3000.565		3000.58
		3008.814		3008.89
		3008.994		3009.07
$v_2 + v_6$	0	2999.922	2999.9	2999.92
	1	3002.313		3002.31
		3011.446		3011.45
		3011.611		3011.62

Figure 1: The coordinate system defined by $(N-1)$ orthogonal polyspherical vectors $\mathbf{r}_i$ in the body-fixed (BF) frame. The BF z-axis is chosen to be coincident with the vector $\mathbf{r}_{N-1}$ while the vector $\mathbf{r}_{N-2}$ lies in the positive xz-plane. The vectors can be a combination of Jacobi, Radau, and orthogonal satellite vectors.

Figure 2: The (3+1) Radau and Jacobi coordinates (Icd=3)[15] for H_2CO, where $\mathbf{r}_1 - \mathbf{r}_3$ are the Radau vectors with respect to atom C and $\mathbf{r}_4$ is the Jacobi vector from the center-of-mass of CH_2G to the O atom. G is a dummy atom with a mass of zero.

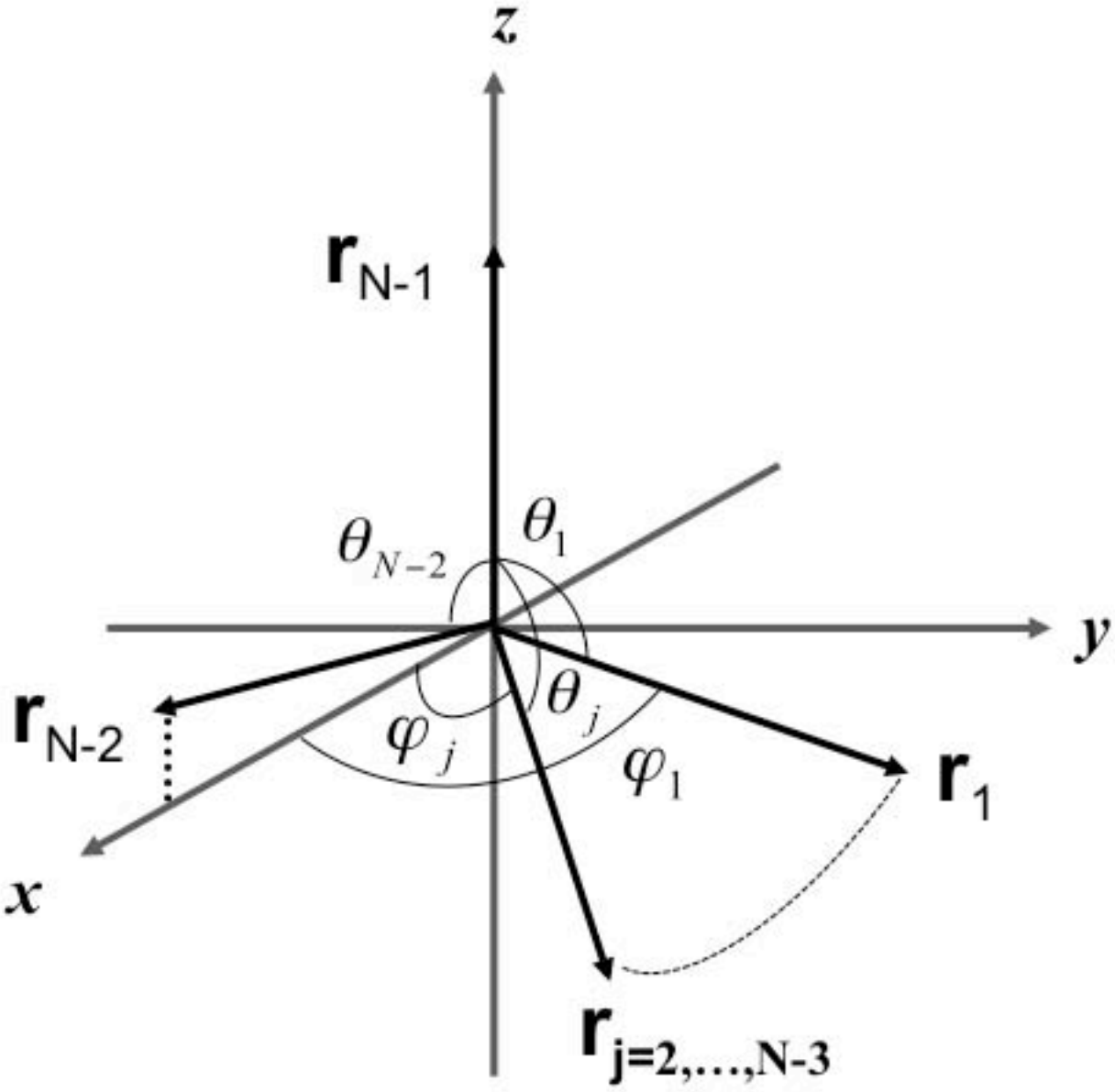
z
r N-1
θ N-2
θ 1
y
r N-2
θ j
φ j
φ 1
r 1
x
r j=2,…,N-3

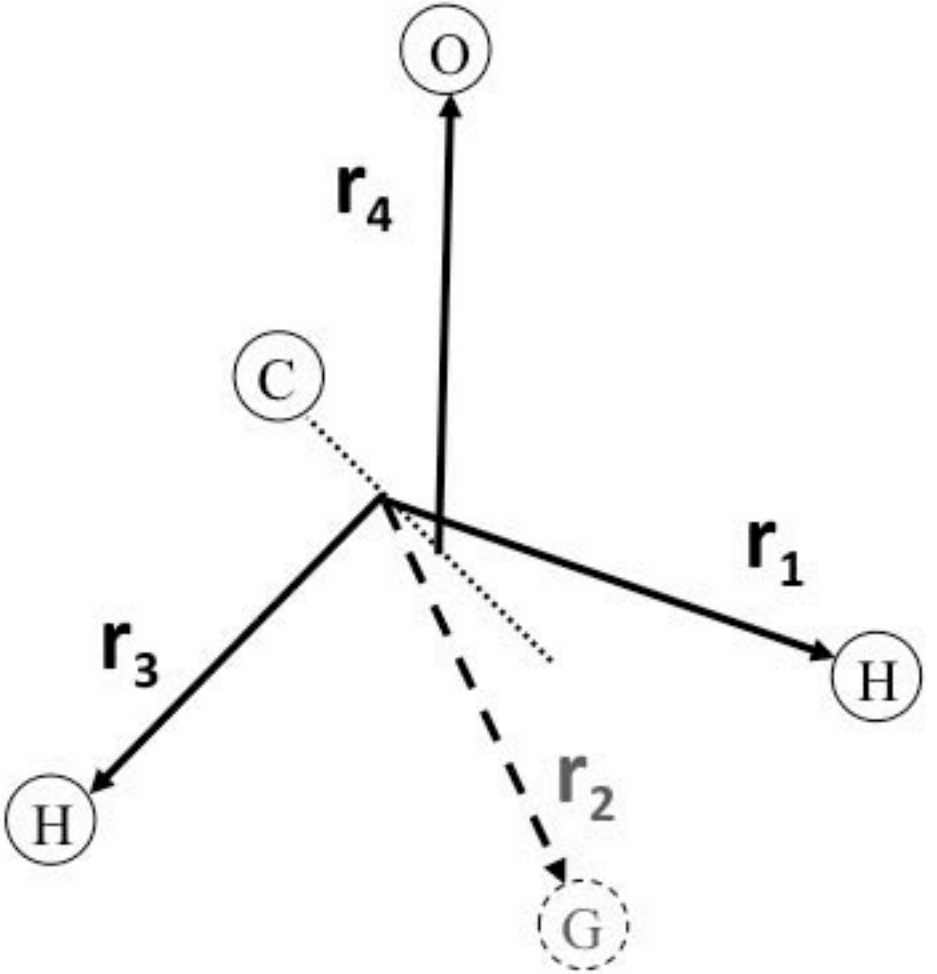
O
r4
C
r1
r3
H
H
r2
G